Springer Series in Geomechanics and Geoengineering

Ancuța Rotaru *Editor*

Knowledge Transfer in the Sustainable Rehabilitation and Risk Management of the Built Environment

KNOW-RE-BUILT. Proceedings of the Online International Multiplier Event/Conference, December 15–16, 2021

Springer

Springer Series in Geomechanics and Geoengineering

Series Editor
Wei Wu, Universität für Bodenkultur, Vienna, Austria

Geomechanics deals with the application of the principle of mechanics to geomaterials including experimental, analytical and numerical investigations into the mechanical, physical, hydraulic and thermal properties of geomaterials as multiphase media. Geoengineering covers a wide range of engineering disciplines related to geomaterials from traditional to emerging areas.

The objective of the book series is to publish monographs, handbooks, workshop proceedings and textbooks. The book series is intended to cover both the state-of-the-art and the recent developments in geomechanics and geoengineering. Besides researchers, the series provides valuable references for engineering practitioners and graduate students.

Indexed by SCOPUS, EI Compendex, INSPEC, SCImago.

Ancuța Rotaru
Editor

Knowledge Transfer in the Sustainable Rehabilitation and Risk Management of the Built Environment

KNOW-RE-BUILT. Proceedings of the Online International Multiplier Event/Conference, December 15–16, 2021

Springer

Editor
Ancuța Rotaru
Transportation Infrastructures
and Foundations Department
“Gheorghe Asachi” Technical University
of Iași
Iași, Romania

ISSN 1866-8755 ISSN 1866-8763 (electronic)
Springer Series in Geomechanics and Geoengineering
ISBN 978-3-031-43454-9 ISBN 978-3-031-43455-6 (eBook)
https://doi.org/10.1007/978-3-031-43455-6

© The Editor(s) (if applicable) and The Author(s), under exclusive license to Springer Nature Switzerland AG 2024

This work is subject to copyright. All rights are solely and exclusively licensed by the Publisher, whether the whole or part of the material is concerned, specifically the rights of translation, reprinting, reuse of illustrations, recitation, broadcasting, reproduction on microfilms or in any other physical way, and transmission or information storage and retrieval, electronic adaptation, computer software, or by similar or dissimilar methodology now known or hereafter developed.
The use of general descriptive names, registered names, trademarks, service marks, etc. in this publication does not imply, even in the absence of a specific statement, that such names are exempt from the relevant protective laws and regulations and therefore free for general use.
The publisher, the authors and the editors are safe to assume that the advice and information in this book are believed to be true and accurate at the date of publication. Neither the publisher nor the authors or the editors give a warranty, expressed or implied, with respect to the material contained herein or for any errors or omissions that may have been made. The publisher remains neutral with regard to jurisdictional claims in published maps and institutional affiliations.

This Springer imprint is published by the registered company Springer Nature Switzerland AG
The registered company address is: Gewerbestrasse 11, 6330 Cham, Switzerland

Paper in this product is recyclable.

Prologue

The International Conference *Critical Thinking in the Sustainable Rehabilitation and Risk Management of the Built Environment—CRIT-RE-BUILT* held in Iași, Romania, in November 2019, brought together participants from many countries around the world and paved the way for a critical analysis of the built environment. Based on the European project entitled Rehabilitation of the Built Environment in the Context of Smart City and Sustainable Development Concepts for Knowledge Transfer and Lifelong Learning (RE-BUILT)—Erasmus+ KA2 programme for Higher education strategic partnerships, it enabled a Springer book with a similar title to grow up and be published. It also seemed to be at that time the inspiration point for the next multiplier event for project outcome dissemination in the form of the International Conference *Knowledge Transfer in the Sustainable Rehabilitation and Risk Management of the Built Environment*, predicted to take place in Vienna in 2021. Four months later, the COVID-19 pandemic shut down the world.

For 16 months, the project partners hoped things would change and longed to come back to normal, but this only happened in mid-2021. From July 2021, with the return to project activities, it was a challenge against time and pandemic for us. Our hope was to organise the planned scientific event in person and produce this book. Sometimes, unfulfilment has to happen before good things can, so the outbreak made travel to Vienna impossible at the end of November 2021 and that was a moment of decision. Due to the deadline imposed by the project, the scientific multiplier event would either take place before the end of the year or not at all.

"Consult not your fears but your hopes and dreams. Think not about your frustrations, but your unfulfilled potential. Concern yourself not with what you tried and failed in, but with what it is still possible for you to do", Pope John XXIII said. And this is what the project partners and the authors of the articles of this book did. In less than two weeks, the scientific event was organised online and took place on 15–16 December 2021. Working on a tight deadline, around 60 authors, most of them being partners in the project, but also some from different parts of the world, presented their works providing knowledge transfer and a range of perspectives to challenge the audience and provoke further ideas and arguments, especially around issues at the intersection of risk management and sustainable rehabilitation of the built environment. Their presentations, which the readers of this book can find in the form of scientific papers, were not only facilitating the close liaison between the knowledge source and the reader but their role can also be strongly associated with practices of translation and interpretation, particularly significant for the knowledge transfer in the built environment domain. A big thanks to all of them!

This book contains 48 papers presented at the RE-BUILT International Multiplier Event *Knowledge Transfer in the Sustainable Rehabilitation and Risk Management of the Built Environment—KNOW-RE-BUILT* held online on 15–16 December 2021. This book specifically retains the main themes analysed in the book entitled *Critical Thinking in the Sustainable Rehabilitation and Risk Management of the Built Environment—CRIT-RE-BUILT*, also published in *Springer Series in Geotechnics and Geoengineering*. By comparison, the replacement of the part "Energy Efficiency. Smart Cities" with "Energy Efficiency. Rehabilitation of the Built Environment" and its unification with the part "Transformation of the Built Environment for the Rehabilitation of Socially Disadvantaged City Districts" are the only changes in the structure of this book.

Hence, the book sets up seven parts that highlight the need to insert knowledge transfer experience into built environment design. It includes knowledge transfer in hazard risk mitigation, sustainable infrastructure design and maintenance, the durability of building materials and structures, rehabilitation in architecture and urban development, building vulnerability and seismic survey, energy efficiency, rehabilitation of the built environment, and conservation of cultural heritage.

Six of the eight European academic teams jointly working on the mentioned project committed to contributing to the refinement of the papers published in the current book by appointing reviewers. In the listing below, the number written in brackets after each reviewer's name shows the number of reviewed papers:

Dr. George Țăranu (5), Dr. Radu-Aurel Pescaru (4), Dr. Ionuț-Ovidiu Toma (4), Dr. Ioana Olteanu (4), Dr. Vasile-Mircea Venghiac (3), Dr. Florin Bejan (2), Dr. Cerasela-Panseluța Neagu (1) from The "Gheorghe Asachi" Technical University of Iași, Romania; Prof. Mauro D'Apuzzo (4), Dr. Andrea Caporale (4), Dr. Azzurra Evangelisti (4), Dr. Ernesto Grande (3), Dr. Valentina Tomei (3), Dr. Luca Paolella (3), Prof. Maura Imbimbo (2), Dr. Giuseppe Modoni (2), Dr. Valentina Cima (2), Dr. Daniela Santilli (2), Dr. Erminio Salvatore (1) within or representing The University of Cassino and Southern Lazio, Italy; Dr. Jan Štefaňák (4), Dr. Jiří Boštík (3), Dr. Alexandra Erbenová (3), Eng. Pavel Koudela (3), Dr. Augustin Leiter (1) from Brno University of Technology, Czech Republic; Prof. Chavdar Kolev (3), Prof. Kiril Angelov (3), Prof. Ivanka Paskaleva (3), Prof. Andrej Totsev (3), Dr. Teodor Berov (3) within or representing The Higher School of Transport Sofia, Bulgaria; Dr. Kaja Pogačar (3), Dr. Peter Šenk (3), Dr. Andrej Tibaut (3), Dr. Sara Guerra de Oliveira (2) from The University of Maribor, Slovenia; Dr. Elise Rémond (4), Prof. Sébastien Rémond (3), Dr. Duc Phi Do (3), Dr. Naima Belayachi (3), Dr. Xavier Brunetaud (1), Dr. Kévin Beck (1) from The University of Orléans, France.

Heartfelt thanks to all reviewers for their valuable contributions in identifying and evaluating key ideas, sources of information, and arguments in the papers included in this volume.

Many thanks to all readers who, interested in sharing knowledge in essential areas of civil engineering, prove their willingness to solve some of the significant challenges of in the sustainable built environment, from reducing the hazard risk to enhancing the sustainable rehabilitation in the field.

With insights for a wide range of readers, ranging from students to professional designers, the book looks at finding successful solutions to all kinds of problems related to hazard risk mitigation and sustainable rehabilitation of the built environment through knowledge transfer. It explores themes such as material design, the vulnerability and durability of building structures, and the power to establish a constructed identity in environmental works. In a way, this book is a manifesto. On the one hand, it advocates structural design and risk management as a bulwark against an increasingly depersonalised built environment, and on the other hand, it prepares answers to the question “But what about the future”?

Iași, Romania Ancuța Rotaru

Contents

Hazard Risk Mitigation for a Sustainable Built Environment

Sustainable Infrastructure Design and Maintenance

The Durability of Sustainable Materials and Structures

Sustainable Rehabilitation in Architecture and Urban Development

Vulnerability, Seismic Survey and HBIM-Based Structural Analysis

Energy Efficiency. Rehabilitation of the Built Environment

Conservation, Rehabilitation and Integration of Cultural Heritage

Hazard Risk Mitigation for a Sustainable Built Environment

Modelling of Critical Slip Surface Geometry for Sustainable Slope Stability Analysis

Ancuța Rotaru and Florin Bejan

1 Introduction

A landslide is the gravitational movement of a mass of soil, rock, or debris along a slope. Landslides may be ignored if they do not occur in areas of human interest. However, when they occur on roads, agricultural land, and inhabited areas, they lead to loss of life and property. According to the World Health Organization, an estimated 4.8 million people were affected by landslides worldwide between 1998 and 2017 [1]. A global dataset of fatal aseismic landslides covering the period from January 2004 to December 2016 showed a total of 55,887 deaths in 4862 different landslide events [2].

Romania has never been exempted from the incidence of natural disasters and catastrophes. In Romania, the area at risk of landslides is about 800,000 ha, with more than 50,000 households and 250,000 people. Romania's national sustainable development strategy, formulated in 1998, recognizes the existence of landslides and floods for which preventive measures must be taken (Official Gazette, X 354/16.09.1998).

Slope stability is mainly analysed using the limit equilibrium methods (LEMs) based on force or/and moment of equilibrium. Modern LEM-based software solves problems with complex stratigraphy, uncommon pore water pressure conditions, arbitrary slip surface shapes, concentrated loads, and structural reinforcement. The main limitation of LEMs, is that the soil mass slides along an assumed slip surface without considering soil mass deformations or strains. Theoretically, the finite element methods (FEMs), based on the stress–strain relationships, provide a comprehensive answer to the slope stability problem [3–5].

A. Rotaru · F. Bejan (✉)
Department of Transportation Infrastructure and Foundations, Faculty of Civil Engineering and Building Services, "Gheorghe Asachi" Technical University of Iași, 1 Prof. Dr. Doc. Dimitrie Mangeron St., 700050 Iași, Romania
e-mail: florin.bejan@academic.tuiasi.ro

A. Rotaru (ed.), *Knowledge Transfer in the Sustainable Rehabilitation and Risk Management of the Built Environment*, Springer Series in Geomechanics and Geoengineering, https://doi.org/10.1007/978-3-031-43455-6_1

This paper focuses on analysing slope stability using both LEM and FEM type methods to determine the location and shape of the critical slip surface.

2 Methods

Limit Equilibrium Methods

Limit equilibrium methods (LEMs) investigate the equilibrium of the soil mass prone to slide down under the influence of gravity. Translational or rotational movement is considered on an assumed slip surface below the soil mass. All LEMs are based on the comparison of moments, forces, or stresses that resist soil mass motion with those that can cause unstable motion. The output of the analysis is a factor of safety, defined as the ratio of the shear strength to the shear stress required for equilibrium [6].

The method of slices is the most popular limit equilibrium technique. Several versions of the method are used. These variations can lead to different results due to different assumptions and inter-slice boundary conditions (Fig. 1).

The Ordinary or Swedish method of slices satisfies the moment of equilibrium but not the horizontal or vertical force equilibrium [7]. The Modified Bishop's method satisfies the moment of equilibrium and vertical force equilibrium but does not satisfy horizontal force equilibrium under both drained and undrained loading conditions [8]. Janbu's generalized method of slices satisfies all equilibrium conditions and allows a variety of numerical problems [9]. Morgenstern and Price's method satisfies all equilibrium conditions and allows varied side force orientations [10, 11]. Spencer's method satisfies all equilibrium conditions and assumes that the side forces are parallel [12].

Fig. 1 Method of slices

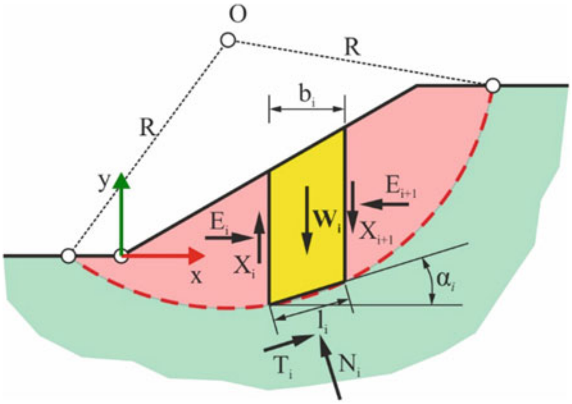

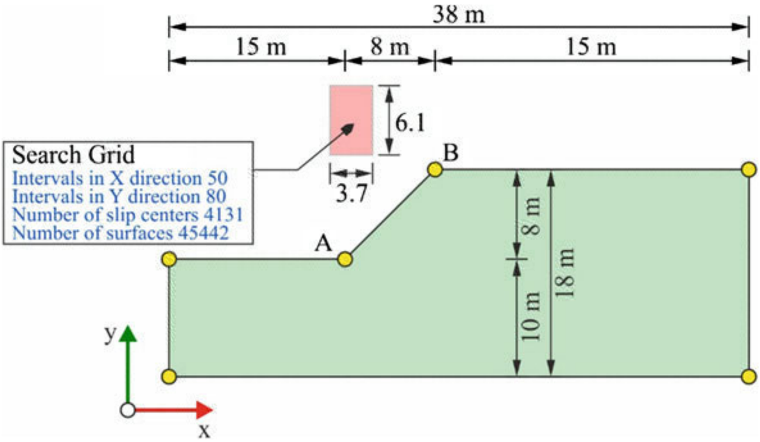

Fig. 2 Slope stability model generated in Slide2 (1:1, H = 8.00 m)

The Slide2 software from Rocscience is used for slope stability analysis using the Ordinary (Fellenius), Bishop, Janbu, Morgenstern–Price and Spencer limit equilibrium methods. The Grid Search Method is used to determine the global minimum safety factor for circular slip surfaces [13, 14]. Figure 2 presents the model for analyzing the slope stability generated in Slide2.

The slip centre grid, which specifies the number of grid intervals, was set to 50 × 80 in the X and Y directions, producing a regular grid of slip centres. Each centre in the slip centre grid represents the centre of rotation of a series of slip circles. The location of the critical slip surface is the one with the lowest value of the factor of safety in the range of assumed surfaces.

Finite Element Method

The finite element method (FEM) uses the shear strength reduction procedure (SSR) to estimate the safety factor using elasto-plastic finite element analysis to gradually decrease the soil strength variables until failure. In this strategy, the strength parameters of the constitutive model for describing the soil behaviour are simultaneously diminished by the same factor up to the slope failure [15]. The factor by which the strength parameters are reduced at the moment of failure represents the factor of safety (FoS).

For the finite element analysis, the Plaxis2D software was used [16, 17]. The selection of the numerical model imposes horizontal and vertical dimensions large enough to avoid boundary perturbation on the results of slope stability analysis. The geometry of the model was set to 60 m × 35 m (Fig. 3).

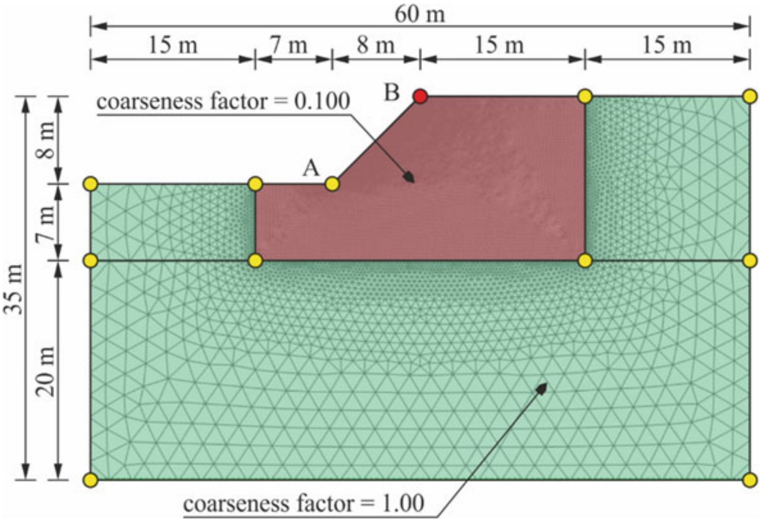

Fig. 3 Slope stability model generated in Plaxis2D (1:1, H = 8 m) 6.21

The analysis used the Mohr–Coulomb failure criterion with a perfect plastic flow with no plastic dilatancy. All analysed cases operate with plane strains and 15-node triangular elements. The mesh coarseness was set to "very fine". Near the slope (red area), the discretization was thickened by a factor of 0.1 (Fig. 3). The purpose of using a fine mesh is to model the shape of the critical slip surface with high accuracy concerning the picked-up points.

Methodology for Identification of the Location and Shape of the Slipping Surface in FEM Analysis

The finite element method does not explicitly specify the position and shape of the critical slip surface. Therefore, from the relative deformation graph, a series of points with relative displacement $|\Delta u|$ equal to zero, located near areas with large relative displacements, were selected (Fig. 4).

The point coordinates collected by Plaxis were centralized in an Excel file and modelled using four types of regression curves: circle, damped sinusoid, second-degree parabola and logarithmic spiral.

For Shape 1, the equation of the circle (Eq. 1) was considered.

$$R_{FIT} = \sqrt{(x - X_C)^2 + (y - Y_C)^2} \tag{1}$$

where, X_C and Y_C are the coordinates of the centre of the circle.

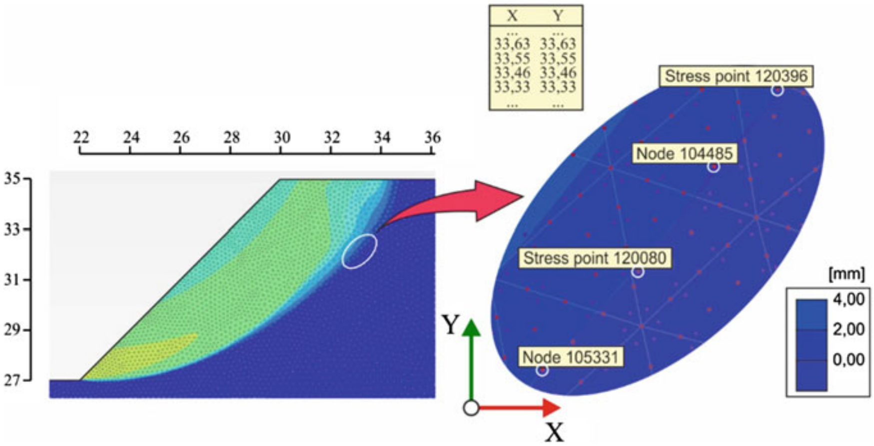

Fig. 4 Scheme for selecting points from the incremental displacements |Δu| graph modelling the shape of the critical failure surface

For Shape 2, the equation of a damped sinusoid (Eq. 2) was considered.

$$Y_{FIT} = A \cdot e^{-\gamma \cdot X} \cdot \cos(\omega \cdot X + \phi) - B \tag{2}$$

For Shape 3, the equation of a second-degree parabola (Eq. 3) was considered.

$$Y_{FIT} = A \cdot X^2 + B \cdot x + C \tag{3}$$

For Shape 4 the equation of a logarithmic spiral (Eq. 4) was considered.

$$r_{FIT} = A \cdot e^{B \cdot \theta} \tag{4}$$

$$\theta = a\sin\left(\frac{Y_C - Y}{r}\right) \tag{5}$$

$$r = \sqrt{(X_C - X)^2 + (Y_C - Y)^2} \tag{6}$$

The approach used to find the coefficients that minimize the error of these models was the least-squares optimization.

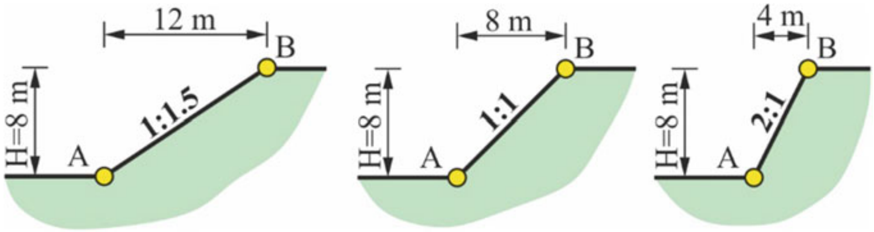

Fig. 5 The geometry of selected slopes

Table 1 Geotechnical characteristics of soils

Type of soil	γ (kN/m^3)	c' (kPa)	ϕ' (°)
S1—clayey silt	18.0	10	18
S2—sandy-clayey silt	19.0	15	20
S3—sandy-silty clay	19.5	20	24
S4—clay	20.0	40	20

3 Results

Case Studies for the Comparative Study

This paper proposes the calculus of three slope gradients (Fig. 5) and four types of homogeneous soils with specific properties (Table 1) using five limit equilibrium methods and the shear strength reduction method.

In the limit equilibrium method, the shape of the critical slip surface is assumed to be circular and the Slide2 program automatically provides the position of the centre and the radius R defined by the X_C and Y_C coordinates. Tables 2, 3 and 4 show the values of the safety factors and the parameters characterizing the critical slip surface (X_C, Y_C and R) obtained using the five limit equilibrium methods (Fellenius, Bishop simplified, Janbu corrected, Spencer and Morgenstern–Price) for the 12 considered slopes.

In Plaxis2D, the slope yields through the phi-c reduction procedure if the safety factor is greater than 1.00. When the stability factor is less than 1.00 (Slope 1:1, H = 8.00 m, S1; Slope 2:1, H = 8.00 m, S1; Slope 2:1, H = 8.00 m, S2), the slope yields from gravitational loading (Initial Phase). In all these cases, the problem of determining the position and shape of the critical slip surface is reduced to extracting the points on the band of “0”, following the slip surface (Fig. 4), from the incremental deformation diagram. The coordinates of these points were centralized in an Excel file and modelled using equations for four types of curves: circle, damped sinusoid, second-degree parabola and logarithmic spiral. The constants of these equations were obtained using the least-squares method. Constant values for the circle (X_C, Y_C, and

Table 2 Results for a 1:1.5 slope, H = 8.0 m

Soil type		S1				S2			
Method		FoS	X_C	Y_C	R	FoS	X_C	Y_C	R
LEM (Slide)	Fellenius	1.17	2.27	13.97	14.16	1.46	2.71	13.36	13.64
	Bishop simplified	1.22	1.39	15.04	15.10	1.53	1.98	14.35	14.49
	Janbu corrected	1.22	1.97	14.35	14.49	1.53	2.56	13.59	13.83
	Spencer	1.22	1.39	15.04	15.10	1.53	1.98	14.35	14.49
	Morgenstern–Price	1.22	1.39	15.04	15.10	1.53	1.98	14.35	14.49
FEM (Plaxis)		1.19	1.16	17.48	17.71	1.51	1.86	16.74	17.02
Soil type		S3				S4			
Method		FoS	X_C	Y_C	R	FoS	X_C	Y_C	R
LEM (Slide)	Fellenius	1.84	2.93	13.06	13.38	2.51	3.96	11.23	11.91
	Bishop simplified	1.93	2.05	14.28	14.42	2.60	3.74	11.69	12.27
	Janbu corrected	1.91	2.56	13.59	13.83	2.66	3.66	11.84	12.39
	Spencer	1.92	2.05	14.28	14.42	2.60	3.59	11.99	12.51
	Morgenstern–Price	1.92	2.05	14.28	14.42	2.60	3.74	11.68	12.27
FEM (Plaxis)		1.84	3.14	14.85	15.91	2.60	3.92	14.85	15.91

Table 3 Results for a 1:1 slope, H = 8.0 m

Soil type		S1				S2			
Method		FoS	X_C	Y_C	R	FoS	X_C	Y_C	R
LEM (Slide)	Fellenius	0.96	– 0.75	12.24	12.26	1.22	– 0.02	11.78	11.77
	Bishop simplified	0.99	– 1.04	12.39	12.43	1.26	– 0.39	12.01	12.01
	Janbu corrected	1.01	– 0.90	12.31	12.34	1.29	– 0.39	12.01	12.01
	Spencer	0.99	– 1.06	12.39	12.43	1.26	– 0.39	12.01	12.01
	Morgenstern–Price	0.99	– 0.97	12.39	12.41	1.26	– 0.46	12.08	12.08
FEM (Plaxis)		0.94	– 2.21	15.20	15.38	1.19	– 1.72	14.47	14.71
Soil type		S3				S4			
Method		FoS	X_C	Y_C	R	FoS	X_C	Y_C	R
LEM (Slide)	Fellenius	1.54	– 0.02	11.78	11.77	2.19	1.46	10.52	11.02
	Bishop simplified	1.59	– 0.39	12.01	12.01	2.23	0.95	10.97	11.02
	Janbu corrected	1.63	– 0.39	12.01	12.01	2.35	0.14	14.78	14.79
	Spencer	1.59	– 0.39	12.01	12.01	2.22	1.32	10.67	10.74
	Morgenstern–Price	1.59	– 0.39	12.01	12.01	2.22	0.95	10.97	11.02
FEM (Plaxis)		1.50	– 1.32	13.79	13.94	2.13	0.03	14.44	14.54

Table 4 Results for a 2:1 slope, H = 8.0 m

Soil type		S1				S2			
Method		FoS	X_C	Y_C	R	FoS	X_C	Y_C	R
LEM (Slide)	Fellenius	0.74	– 4.06	10.17	10.95	0.96	– 3.62	10.32	10.93
	Bishop simplified	0.74	– 2.96	8.72	9.21	0.95	– 2.81	8.72	9.16
	Janbu corrected	0.79	– 4.57	11.54	12.40	1.02	– 4.43	11.62	12.43
	Spencer	0.76	– 4.21	11.85	12.54	1.01	– 3.11	12.38	12.76
	Morgenstern–Price	0.77	– 3.99	11.92	12.56	1.01	– 3.11	12.46	12.81
FEM (Plaxis)		0.60	– 7.83	17.39	19.13	0.89	– 7.20	16.03	17.66
Soil type		S3				S4			
Method		FoS	X_C	Y_C	R	FoS	X_C	Y_C	R
LEM (Slide)	Fellenius	1.22	– 4.43	11.62	12.43	1.80	– 1.75	10.46	10.60
	Bishop simplified	1.21	– 2.74	8.72	9.13	1.76	– 1.16	8.33	8.41
	Janbu corrected	1.30	– 4.43	11.62	12.43	1.96	– 2.99	12.44	12.79
	Spencer	1.30	– 2.81	12.53	12.83	2.04	0.08	13.51	13.50
	Morgenstern–Price	1.29	– 2.89	12.53	12.84	2.01	– 0.13	13.51	13.49
FEM (Plaxis)		1.17	– 7.38	15.78	17.50	1.79	– 3.97	14.84	15.49

R) are presented in Tables 2, 3, and 4 and constant values for the other types of curves are shown in Table 5.

Figure 6 shows the positions of the critical failure surfaces with a 1:1.5 slope obtained using the limit equilibrium methods and the finite element method. Both categories of methods consider a circular slip surface. There are no significant differences between the critical slip surface positions using the five limit equilibrium methods. The radius of the circle that characterizes the critical failure surface is 19–33% larger in the case of FEM than in the LEMs although the safety factor values are almost the same.

Figure 7 shows the critical slip surfaces of a 1:1 slope obtained using LEMs and FEM. Except for the soil S1, in all the other cases the surfaces have approximately the same position regardless of the method used, although the radii of the circles obtained with FEM are 19–32% larger than those achieved with LEMs.

Figure 8 shows the critical slip surfaces of a 2:1 slope determined using LEMs and FEM.

Again, the radii of the critical slip surfaces for 2:1 slopes obtained with FEM are larger than those obtained using LEMs. A large variation in the position of the critical slip surfaces is also observed between all LEMs.

Table 5 provides the fitting parameters for the damped sinusoid, second-degree parabola and logarithmic spiral for the study cases.

Table 6 provides the fitting error values for each curve type to conclude which model is more suitable for critical failure surface characterization.

In general, the damped sinusoid best fits the results obtained with analysed slopes (bolded values from Table 6). However, in some cases, the logarithmic spiral and

Table 5 Fitting parameters for the damped sinusoid, second-degree parabola and logarithmic spiral for all study cases

Slope	Soil type	Shape 2 damped sinusoid					Shape 3 parabola			Shape 4 log-spiral			
		A	ω	ϕ	γ	B	A	B	C	X_C	Y_C	A	B
1:1.5	S1	29.06	− 0.04	− 10.14	− 0.04	− 21.81	0.04	− 0.22	0.06	2.18	19.48	16.87	0.10
	S2	− 28.75	0.04	− 11.89	− 0.04	− 22.40	0.04	− 0.27	0.07	2.64	18.81	16.50	0.10
	S3	43.74	− 0.05	3.69	0.02	− 36.20	0.04	− 0.27	− 1.14	3.88	27.46	21.03	0.22
	S4	32.85	− 0.04	2.87	− 0.02	− 31.17	0.05	− 0.43	− 0.34	4.31	18.74	16.25	0.14
1:1	S1	28.19	0.06	3.63	− 0.03	− 25.10	0.06	− 0.06	0.21	− 0.09	16.78	12.97	0.17
	S2	32.27	0.05	3.61	0.03	− 28.80	0.06	− 0.07	0.05	0.88	16.73	11.74	0.23
	S3	8.09	0.05	4.33	− 0.10	− 2.98	0.07	− 0.14	0.19	0.83	15.57	11.49	0.20
	S4	7.93	0.00	4.79	− 0.21	0.82	0.06	− 0.20	0.17	1.05	15.29	13.39	0.09
2:1	S1	4.20	0.02	7.55	− 0.34	1.18	0.07	0.29	0.08	− 2.29	20.73	12.54	0.35
	S2	3.34	0.03	13.81	− 0.37	1.02	0.08	0.25	0.08	− 2.25	19.39	11.82	0.35
	S3	1.14	− 0.09	12.08	− 0.36	0.95	0.08	0.27	0.07	− 2.86	19.26	12.21	0.33
	S4	1.15	− 0.04	5.29	− 0.37	0.63	0.07	0.05	0.09	0.49	18.06	10.29	0.36

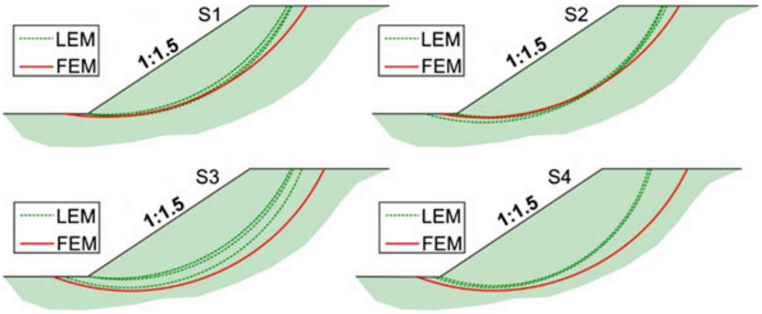

Fig. 6 Location and shapes of the critical slip surface of a 1:1.5 slope determined using LEMs and FEM

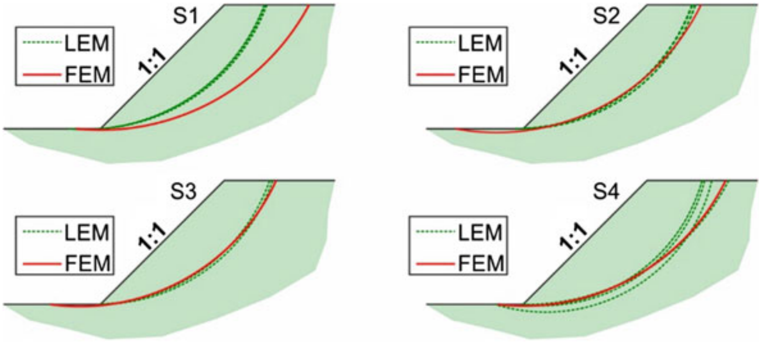

Fig. 7 Location and shapes of the critical slip surface of a 1:1 slope determined using LEMs and FEM

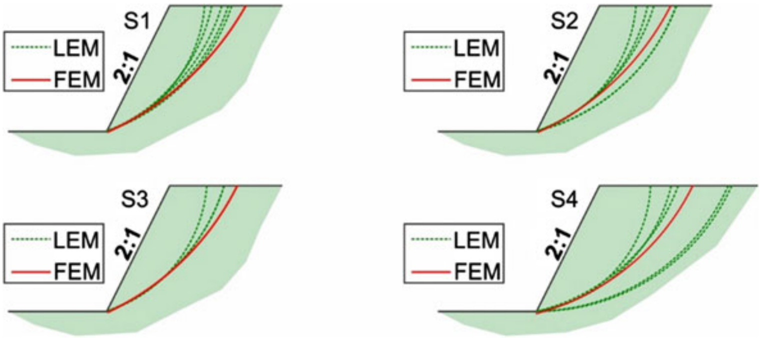

Fig. 8 Location and shapes of the critical slip surface of a 2:1 slope determined using LEMs and FEM

Table 6 Fitting errors of regression curves for the four curve models of the critical slip surface

Slope	Soil type	Fitting shape			
		Shape 1	Shape 2	Shape 3	Shape 4
1:1.5	S1	0.573	**0.146**	0.527	0.240
	S2	0.792	**0.207**	0.682	0.400
	S3	9.166	**0.808**	1.752	1.923
	S4	4.831	**0.745**	1.140	1.383
1:1	S1	0.388	**0.218**	0.379	0.305
	S2	0.895	1.485	1.704	**0.609**
	S3	0.696	0.800	1.354	**0.418**
	S4	1.750	2.132	3.572	**1.335**
2:1	S1	0.706	**0.069**	0.187	0.444
	S2	1.036	**0.061**	0.207	0.623
	S3	1.237	**0.038**	0.183	0.764
	S4	1.537	**0.116**	0.341	0.778

Shape 1—circle, Shape 2—damped sinusoid, Shape 3—second-degree parabola, Shape 4—log-spiral

second degree parabola fit best. The circular surface does not seem to confirm any case taken into account.

4 Conclusions

In this study, limit equilibrium analysis and finite element analyses were performed using Slide2 and Plaxis, respectively. Both software are powerful tools for assessing slope stability. Slide2 uses the limit equilibrium method and Plaxis uses the finite element method. An important limitation of the conventional limit equilibrium methods is the need to assign the geometry of potential failure surface before performing the calculations. In the finite element method, the location and shape of the potential slip surface is not determined before the analysis. Therefore, in this study, a methodology was proposed and used to determine the position and shape of the critical slip surface using finite element method results.

The analysis was performed on homogenous 8.00 m height slopes with three distinct gradients (1:1.5; 1:1; 2:1) and four different soil properties (S1–S4). The position and shape of the critical slip surface were obtained from both types of methods. The results presented in this study showed that the damped sinusoidal model generally fits the critical slip surface best.

The results presented in this study may serve as a starting point for further research on the geometry of the critical slip surface. They should further progress to provide relevant interpretations, summarized in the form of regression curves of several other shapes, where the most probable shape of the critical slip surface was defined using various equations.

References

1. World Health Organization. https://www.who.int/health-topics/landslides#tab=tab_1. Accessed 21 Nov 2019
2. Froude MJ, Petley DN (2018) Global fatal landslide occurrence from 2004 to 2016. Nat Hazards Earth Syst Sci 18:2161–2181
3. Burman A, Acharya SP, Sahay RR, Maity D (2015) A comparative study of slope stability analysis using traditional limit equilibrium method and finite element method. Asian J Civil Eng AJCE 16(4):467–492. ISSN: 1563-0854
4. Sami U, Muhib UK, Gohar R (2020) A brief review of the slope stability analysis methods. Geol Behav (GBR) 4(2):73–77
5. Senapati S, Senapati S (2021) Comparison of LEM and FEM based solution for slope stability analysis using soilworks. In: Biswas S, Metya S, Kumar S, Samui P (eds) Advances in sustainable construction materials. Lecture notes in civil engineering, vol 124. Springer, Singapore
6. Salunkhe DP, Chvan G, Bartakke RN, Kothavale PR (2017) An overview on methods for slope stability analysis. IJERT 6:528–535
7. Fellenius W (1936) Calculation of the stability of earth dams. In: Transactions of the 2nd congress on large dams. International Commission on Large Dams (ICOLD), Washington, DC, Paris, pp 445–462
8. Bishop AW (1955) The use of slip circle in the stability analysis of earth slopes. Geotechnique 5:7–17
9. Janbu N (1954) Application of composite slip surfaces for stability analysis. In: Proceedings of the European conference on stability of earth slopes 1954, vol 3, Stockholm, pp 43–49
10. Morgenstern NR, Price VE (1965) The analysis of the stability of general slip surfaces. Geotechnique 15:79–93
11. Morgenstern NR, Price VE (1967) A numerical method for solving the equations of stability of general slip surfaces. Comput J 9:388–393
12. Spencer E (1967) A method of analysis of the stability of embankments assuming parallel interslice forces. Geotechnique 17:11–26
13. Rocscience learning resources homepage. https://www.rocscience.com/learning?program=Slide2. Accessed 29 Jan 2022
14. Peng Q, Cong L, Xueming J (2016) The research of high slope instability mechanism based on slide. Am J Civ Eng 4(2):61–67
15. Griffiths DV, Lane PA (1999) Slope stability analysis by finite elements. Geotechnique 49(3):387–403
16. Bentley communities—manuals. Plaxis homepage. https://communities.bentley.com/products/geotech-analysis/w/wiki/46137/manuals---plaxis. Accessed 27 Jan 2022
17. Alex J, Ammu AT, Aparna GN, Arshiq MP (2018) Slope stability analysis using PLAXIS 2D. IRJET 5:3666–3668

Landslide Displacement Prediction with Machine Learning Techniques

Carlotta Guardiani, Enrico Soranzo, David Ottowitz, Birgit Jochum, and Wei Wu

1 Introduction

Strategies for landslide risk mitigation enclose structural and non-structural measures. The Sendai Framework for Disaster Risk Reduction adopted by the United Nations (2015–2030) identifies four priorities and specific key actions to reduce disaster risk [1]. In addressing this objective, early warning systems play a major role concerning the following tasks: understanding disaster risk through monitoring, developing forecasting systems, enhancing disaster preparedness and finally, increasing the resilience of communities.

Early warning systems continuously monitor parameters that are related to landslide movements (e.g., displacement or its derivatives) and their triggering mechanisms. A component of warning models (and of early warning systems) is the landslide model, which conceptually or mathematically describes the relationship between meteorological triggers and landslide events, supported by monitoring data and available historical information (e.g., geological mapping, geotechnical inspections etc.) [2]. Landslide prediction models can be classified into "physics-based" and "data-driven" models. The former describes analytically or numerically the physical process, based on the limit equilibrium theory or the strength reduction method combined with finite element or finite difference methods. The latter includes prediction models based on the creep theory and statistical/artificial intelligence (AI) [3]. The methods based on the creep theory use observations of the displacement rate to

---

C. Guardiani (✉) · E. Soranzo · W. Wu
Institute of Geotechnical Engineering, University of Natural Resources and Life Sciences, Feistmantelstrasse 4, 1180 Vienna, Austria
e-mail: carlotta.guardiani@boku.ac.at

D. Ottowitz · B. Jochum
Department of Near Surface Geophysics, GeoSphere Austria, Hohe Warte 38, 1190 Vienna, Austria

A. Rotaru (ed.), *Knowledge Transfer in the Sustainable Rehabilitation and Risk Management of the Built Environment*, Springer Series in Geomechanics and Geoengineering, https://doi.org/10.1007/978-3-031-43455-6_2

predict the time of failure (e.g., the Saito and Fukozono models [4, 5]). Statistical models (e.g., autoregressive models) and recently AI algorithms employ monitoring data to predict future displacements.

In the last decade, monitoring instrumentation has become highly sophisticated, leading to an abundance of data that cannot be manually processed and interpreted. In this perspective, the recent advances in AI offer the opportunity to take full advantage of the information collected by monitoring sensors. The results of this study represent an initial step for the automatic estimation of warning thresholds and a tool to support experts' judgment before warning dissemination. In this work, we apply machine and deep learning algorithms, namely Support Vector Regression, Extreme Gradient Boosting, and Long Short-Term Memory, on the monitoring data of two case studies, in China and Austria. The methods and algorithms applied are the same for both sites (which differ in geological conditions and triggering factors). However, data preparation needs to be tailored to each specific dataset.

2 Material and Methods

Case Studies

Huangtupo The Huangtupo landslide is the largest active landslide in the Three Gorges Reservoir Region, with an area of 1.35 km^2 and a volume of 70 million m^3. It is situated ca. 70 km upstream of the Three Gorges Dam on the Yangtze River in the county of Badong (Hubei Province). In the last 40 years, the community has been relocated twice. After the first relocation, due to the dam's construction, evidence of landslide instability was found in Huangtupo. This landslide is classified as complex and four separate sliding masses have been identified. The composition consists of mudstone, pelitic siltstone and argillaceous limestone [6]. Since the impoundment of the Three Gorges Reservoir, the toe of the Huangtupo landslide, whose elevation is between 50 and 90 m a.s.l., is submerged by the Yangtze River. The operational level of the reservoir varies between 145 and 175 m a.s.l. throughout the year, leading to the reactivation of large landslides.

In 2012, the China University of Geosciences (Wuhan) completed a comprehensive field test facility for research on landslide hazards in the Three Gorges Reservoir Region. It comprises a tunnel built in the bedrock below the sliding mass called "Riverside Slump I", which exhibited the largest displacements, and other monitoring equipment such as inclinometers, extensometers, and GPS. In this study, we employ the monitoring data from two GPS points located on Riverside Slump I, namely G7 and G9, which are above the thickest sliding zone (G7) and the steepest part of the sliding surface (G9) [7]. To study the relationship between triggering mechanisms and surface displacements, rainfall and reservoir water levels from 2003 until 2011 have also been provided [7]. The data have a monthly frequency, for a total of 100 data points.

Laakirchen In March 2010, after snow melting and heavy rainfall, a shallow rotational landslide occurred in the vicinity of a newly renovated house in Laakirchen (district of Gmunden, Upper Austria). The slope is composed of an 8-m thick layer of coarse excavation soil lying on the weathered geological formation Schlier, which consists of silty or fine-grained marls and calcareous clay. In September 2011, the Geological Survey of Austria installed an automatic inclinometer (D.M.S. [8]) and a geoelectrical system [9] together with a rain gauge for monitoring purposes. In less than two years (until June 2003), a cumulative displacement of ca. 70 mm has been recorded at a depth of 3.5 m b.g.l. by the automatic inclinometer. The inclinometer readings have an hourly frequency. Additional rainfall data from a weather station in the vicinity have been provided by GeoSphere Austria with daily frequency. Therefore, after manual detection and removal of outliers, we have homogenized the overall dataset and resampled it with a daily frequency.

Data Preprocessing

In this section, we present the forecasting procedure. The forecasting problem is set as multivariate, assuming a relationship of dependence between one or more triggering factors and landslide displacements. In machine learning, the independent variables are called features, whereas the target is the variable to be predicted. In this study, we derive the target from the time series of cumulative displacements for both sites, which exhibit an increasing trend. Generally, to improve the forecast, it is recommended to decompose a time series into trend and seasonal components or to transform it into a stationary time-series [10]. Based on the assumption that the trend is controlled by predisposing factors (e.g., geological and lithological conditions) and the seasonal part by external triggers (e.g., intensive rainfall and fluctuations of the reservoir water level for the site of Huangtupo) [11], we decompose the cumulative displacement in an additive manner. This approach has proved successful for landslides with a step-wise evolution and strong seasonality [12]. Alternatively, stationarity can be achieved by differencing a time series, i.e., subtracting consecutive observations. In this way, the cumulative displacements are converted to the displacement rate (or velocity).

The main features are the cumulative rainfall and the reservoir water level (only for the Huangtupo landslide). In machine learning, the operation of extracting additional features is termed “feature engineering”. Especially for univariate forecasting problems (i.e., forecasting a time series using the same variable as feature and target), observations are shifted over time to create lag features. In this study, lag features are produced from all raw time series (e.g., cumulative displacements, cumulative rainfall and reservoir water level), using past observations to predict the actual time step. Other features are calculated from the previous ones, like displacement rates, rainfall during a specific antecedent time window and the variation of the reservoir water level for the Huangtupo landslide. To reduce the effects of the “curse of dimensionality”, feature selection is applied to decrease the number of dimensions of the feature space, for example by ranking the time series according to the highest correlation with the target. In the context of landslide prediction models, Grey Relational Analysis (GRA) has been successfully employed [13]. We apply this technique to time series following the procedure of Sallehuddin et al. [14]. The outcome of this analysis is the grey relational grade (GRG), which indicates the level of correlation between the target time series and the features. A GRG above 0.8 denotes a strong correlation, while values below 0.6 are neglectable.

Cross-validation and hyperparameter tuning. The dataset is divided into a training and a test set, with a train-test split ratio of 80–20%. To avoid overfitting, we perform cross-validation. The training set is split into k folds, among which $k - 1$ are used for training the model and the kth-fold (also called "hold out" set) corresponds to the validation set. This process is repeated for k iterations so that all data of the original training set (80% of the total dataset in this study) are used both for training and validation. However, classical k-fold cross-validation cannot be applied to time series since it would alter the chronological order of the observations. Therefore, training and validation sets with a fixed length are shifted over time, keeping the latter always subsequent to the former. An evaluation score is obtained at each iteration (or shift) and the cross-validation score is the average value of all scores.

Within cross-validation, the best combination of hyperparameters is selected based on the obtained score, while the final evaluation is made exclusively on the test set, which contains unseen data. The first alternative to manual hyperparameter tuning is the grid search method, with which the user defines a set of values for each hyperparameter and trains the model with all possible combinations. This method can be highly time-consuming, especially with many hyperparameters. In this study, hyperparameter optimization is performed with Hyperopt [15], a Python library that provides algorithms for Bayesian optimization. Here, the hyperparameter space is defined as a probability distribution for each hyperparameter to be tuned. We set the root mean square error (RMSE) as the loss function, which is the objective function to minimize. Based on the evaluations of the score with its corresponding hyperparameter value, the Bayesian optimization updates the probability distribution and suggests a new value of the hyperparameter for the next trial. The search algorithm is the Tree-of-Parzen-Estimators (TPE) (more information is available in [16]). In the beginning, this process is rather random and gradually, the algorithm focuses on a more restricted region of the search space with increasing iterations.

Model Selection

Support Vector Regression (SVR). Support Vector regression is an extension of support vector machines for nonlinear regression problems [17]. This model maps data into a high-dimensional feature space (called kernel space) with a function, which can be a nonlinear transformation. In the kernel space, the data are transformed by the kernel function into new linearly separable instances. For regression, a hyperplane is searched to find the narrowest tube that contains most of the data. In this study, the kernel function is the radial basis function (RBF).